Deformed Gazeau-Klauder Schrödinger cat states with modified commutation relations

C. L. Ching[1,*] and W. K. Ng[2,†]

[1]*Science and Math Cluster, Singapore University of Technology and Design (SUTD), Upper Changi 487372, Singapore*

[2]*Department of Physics, National University of Singapore (NUS), Kent Ridge 117551, Singapore*

(Received 9 July 2019; published 25 October 2019)

Generalized coherent states under deformed quantum mechanics that exhibit intrinsic minimum length [Phys. Rev. D **86**, 064038 (2012)] and maximum momentum [Phys. Rev. D **88**, 084009 (2013)] have been well studied following the Gazeau-Klauder approach. In this paper, as an extension to the study of quantum deformation, we investigate the famous Schrödinger cat states (SCs) under these two classes of quantum deformation. Following the concept of generalized Gazeau-Klauder Schrödinger cat states (GKSCs) in [J. Phys. A **45**, 244006 (2012)], we construct the deformed GKSCs for both phenomenological models that exhibit intrinsic minimum length and/or maximum momentum. All comparisons between minimum length and maximum momentum deformations are illustrated and plots are done in even and odd cat states since they are one of the most important classic statistical characteristics of SCs. Probability distribution and entropies are studied. In general, deformed cat states do not possess the original even and odd state statistical properties. Nonclassical properties of the deformed GKSCs are explored in terms of the Mandel Q parameter, quadrature squeezing $(\Delta X_q)\cdot(\Delta Y_q)$, as well as Husimi quasiprobability distribution $\mathcal{Q}$. Some of these distinguishing quantum-gravitational features may possibly be realized qualitatively and even be measured quantitatively in future experiments with the advanced development in quantum atomic and optics technology.

DOI: 10.1103/PhysRevD.100.085018

I. INTRODUCTION

After almost more than half of a century of intense research activities to reconcile the two main pillars of modern physics, namely, quantum mechanical theory, which governs the subatomic world, and general relativity, which describes physics at the cosmological scale, up to date there is still no common consensus on the form of new gravitational effects that may show up in quantum systems at high energy. Nevertheless, there are a few partially promising candidates for a quantum theory of gravity, such as superstrings theory [1,2], loop quantum gravity (LQG) [3,4], noncommutative geometry (NC) [5,6], renormalization group (RG) flow/asymptotic safety [7] approach, etc. All of these approaches predict some important generic physical features such as the existence of a minimal resolution length scale $l_{\min}$, probably the taken value at about the order of Planck length $L_p = \sqrt{\frac{\hbar G}{c^3}} \approx 1.6 \times 10^{-35}$ m [8]. Here $\hbar$ is the Planck constant, G is the Newton gravitational constant, and c is the speed of light. From the phenomenological point of view, modified quantum commutation relations (MCRs) have been extensively studied as effective means of encoding potential gravitational or stringy/loopy effects; see Refs. [9–22] and the reviews [23,24] for a complete list of references. While most of the studied MCRs incorporate a minimum position uncertainty and usually lead to the concept of a minimal length scale thus consistent with quantum gravity phenomenology, there are others that exhibit a maximum momentum; see Refs. [25–38] as in doubly special relativity [39,40] and the anti-Snyder model [9,33]. It has also been suggested that the consequent deformations of quantum mechanical spectra and relevant physics might be detectable in future low-energy experiments [41–47]. In Ref. [38], we investigated in detail large classes of deformed quantum mechanics of the latter type and their implication in quantum optical systems [48]. The current manuscript is an extension to these previous work and inspired by [49].

On the other hand, coherent states (Cs) and squeezed states (Ss) are very interesting quantum systems in nature due to their ability to exhibit the "quantumness" ranging

*Corresponding author.
cheeleong_ching@sutd.edu.sg
†phynwk@nus.edu.sg

from almost classical[1] to highly nonclassical features such as quadrature squeezing below the Heisenberg uncertainty principle (HUP) boundary, sub-Poisonnian statistics, antibunching effects, and quasiprobability distribution; see Refs. [50–60]. These interesting features enable both coherent and squeezed states to be extremely useful in quantum information processing [61,62], optical communication and measurement [63], quantum metrology [64], quantum cryptography [65], etc. Particularly, squeezed states have been used in LIGO to increase the sensitivity of gravitational wave detectors since one can achieve lower noise in spatial quadrature [66,67]. Furthermore, recently there is an increase of interest to study the generalized squeezed state in noncommutative and deformed space settings [48,68–76] in order to capture the nonconventional quantum gravitational effects [47] and also relations to quantum nonlocality [77].

Our manuscript is organized as follows: In Sec. II, we review the formalism of generalized Heisenberg algebra (GHA) [78–80] in constructing the so-called Gazeau-Klauder's coherent states (GKCS) [51,81–83] and further obtain their superposition as the Gazeau-Klauder Schrödinger cat states (GKSCs)[49,72]. In Sec. III, after reviewing the two important quantum gravity inspired phenomenological models that exhibit minimal length and/or maximum momentum scale, we explicitly construct the deformed GKSCs. We study the probability distribution and entropies of the odd and even deformed GKSCs in Sec. IV. The nonclassical behaviors of the cat states are further explored in terms of number and quadrature squeezing in Sec. V, as well as Husimi's distribution in Sec. VI. Finally we conclude in Sec. VII.

II. GAZEAU-KLAUDER COHERENT AND CAT STATES

Cs were first studied by Schrodinger in 1926 in harmonic oscillator systems[84] and later by Klauder and Glauber [50–53,81–83]. Glauber obtained these states in the study of electromagnetic correlation function and realized the interesting feature that these states saturate the HUP, $\Delta x\Delta p = \hbar/2$. Thus, coherent states are considered as quantum states with the closest behavior to the classical system and have many applications in theoretical and mathematical physics [85–87].

In the literature, there are two ways to construct the coherent states. First is through Klauder's approach by using the Fock's representation of ladder algebra and second is the Perelomov-Gilmore's approach [88] based on group theoretic construction. In this paper, we follow Klauder's approach and use the GHA given in [78–80]. In this version of GHA,[2] the Hamiltonian J_0 that is related to the characteristic function $g(x)$ of the physical system, together with ladder operators [$A^\dagger$ being the creation operator and $A = (A^\dagger)^\dagger$ being the annihilation operator], play the role of the generators of the algebra,

$$\begin{aligned} J_0A^\dagger &= A^\dagger g(J_0), \\ AJ_0 &= g(J_0)A, \\ [A^\dagger, A] &= J_0 - g(J_0). \end{aligned} \tag{1}$$

We see that these operators form a closed algebra and $g(J_0)$ is the analytic function of J_0, which is unique for each type of GHA. The Casimir of this algebra is

$$C = A^\dagger A - J_0 = AA^\dagger - g(J_0). \tag{2}$$

The vacuum of the generator J_0 is defined by

$$J_0|0\rangle = \alpha_0|0\rangle, \tag{3}$$

where α_0 is the energy eigenvalue of the vacuum state $|0\rangle$. Also, the vacuum is annihilated by the operator A, i.e., $A|0\rangle = 0$. Consider a general eigenket of J_0, denoted by $|m\rangle$; the generators satisfy the following,

$$\begin{aligned} J_0|m\rangle &= \alpha_m|m\rangle, \\ A^\dagger|m\rangle &= N_m|m+1\rangle, \\ A|m\rangle &= N_{m-1}|m-1\rangle, \end{aligned} \tag{4}$$

where $\alpha_m = g^{(m)}(\alpha_0)$ is the mth iteration of α_0 under g and $N_m^2 = \alpha_{m+1} - \alpha_0$. In [78], it was shown that eigenenergies of any quantum system obey the equation

$$\tilde{\epsilon}_{n+1} = g(\tilde{\epsilon}_n), \tag{5}$$

where $\tilde{\epsilon}_{n+1}$ and $\tilde{\epsilon}_n$ are the eigenenergy of successive energy levels and $g(x)$ is the characteristic function of

[1]Coherent states saturate the HUP in the vacuum state; hence it is regarded as the state closest to classical physics, while Ss showed highly nontrivial quantum randomness in their sub-Poisson distribution and antibunching behavior.

[2]There are other versions of GHA. Back in the early 1950s, E. Wigner posed an intriguing question "Do the equations of motion determine the quantum mechanical commutation relations?" According to Wigner, the equation of motion has a more immediate physical significance than Heisenberg commutation relation $[x_i, p_j] = i\hbar\delta_{ij}$. He found as an answer a generalized quantum mechanical rule (deformation was introduced implicitly here) for the one-dimensional harmonic oscillator [89,90]. Wigner's idea was further explored and it leads to the new deformed quantum commutation relation generally called Wigner-Heisenberg algebra (WHA). This algebra subsequently found many important and interesting physical applications related to quantum chromodynamics [91], parastatistics [92–94], anyons physics [95,96], and supersysmmetry [97]. For recent application of WHA in the context of coherent state, Schrodinger cat states, and quantum entanglement transfer, see Refs. [98–101].

the particular quantum system that satisfies the GHA. For example, one can obtain the standard harmonic oscillator with linear characteristic function $g(x) = x + 1$, the q-deformed oscillator with $g(x) = qx + 1$, and free particle in an infinite square well with $g(x) = (\sqrt{x} + \sqrt{1/2})^2$. In general, GHA may not refer to smooth deformation of Heisenberg algebra [78–80].

Klauder's coherent states are by construction the eigenstates of the family of annihilation operators

$$A(\gamma) = e^{-i\gamma H/(\hbar\omega)} A e^{i\gamma H/(\hbar\omega)},$$
$$A(\gamma)|z,\gamma\rangle = z|z,\gamma\rangle, \tag{6}$$

where $H \equiv J_0$ is the Hamiltonian of the physical system under consideration and $J \equiv |z|^2 \geq 0$ is the average energy in the elementary quantum unit of $\hbar\omega$. z is the complex eigenvalue of the annihilation operators, whereas γ is the real parameter associated with the classical action angle variable [81].

The (temporally stable) Gazeau-Klauder's GKCs are defined as [81]

$$|J,\gamma\rangle = \frac{1}{N(J)} \sum_{n\geq 0} \frac{J^{(n/2)} e^{-i\gamma\epsilon_n}}{\sqrt{\rho_n}} |n\rangle, \qquad \rho_n \coloneqq \prod_{k=1}^{n} \epsilon_k, \tag{7}$$

where we have denoted $\epsilon_n = \frac{\tilde{\epsilon}_n - \tilde{\epsilon}_0}{\hbar\omega}$ and $|n\rangle$ is the number state. $N(J)$ is a normalization constant. For consistency, we set $\rho_0 = 1$. Note that, to ensure that both (J,γ) are action angle variables, we need the GKCs to satisfy

$$\langle J,\gamma|H|J,\gamma\rangle = \hbar\omega J. \tag{8}$$

We have the time independent of expectation value (temporally stable) of Hamiltonian in the state with (J,γ).

The generalized coherent states (GCs) are said to be Gazeau-Klauder's type if they satisfy the following conditions:

(I) Normalizability:

$$|\langle J,\gamma|J,\gamma\rangle|^2 = 1. \tag{9}$$

(II) Continuity in the label:

$$|J - J'| \Rightarrow 0; \||J,\gamma\rangle - |J',\gamma\rangle\| \Rightarrow 0. \tag{10}$$

(III) Completeness:

$$\int (d^2z) w(z,\gamma) |z,\gamma\rangle\langle z,\gamma| = 1, \tag{11}$$

where $(d^2z)w(z,\gamma)$ is the measure on the Hilbert space spanned by $|z,\gamma\rangle$.

The normalization constant can be expressed as

$$|\langle J,\gamma|J,\gamma\rangle|^2 = 1 \Rightarrow N(J)^2 = \sum_{n\geq 0}^{\infty} \frac{J^n}{\rho_n}. \tag{12}$$

Strictly speaking, the GCs exist only if the radius of convergence

$$R = \lim_{n\to\infty} \sup \sqrt[n]{\rho_n} \tag{13}$$

is nonzero [51,82,83]. In fact, different choices of ρ_n and hence the characteristic function $g(\tilde{\epsilon}_n)$ give rise to many different families of GCs. On the other hand, the temporal stability condition of the eigenstates can be obtained by

$$e^{-iHt/\hbar}|z,\gamma\rangle = |z,\gamma + \omega t\rangle. \tag{14}$$

A. GKSCs

Schrödinger cat states (SCs) $|\psi_{sc}\rangle$ are defined as the coherent superposition of the two coherent states $|z\rangle$ and $|-z\rangle$. They have been studied well and their characteristics are summarized in the literatures [55–57]. Although SCs are constructed by coherent state, they are generally nonclassical states where $|z\rangle$ and $|-z\rangle$ can be macroscopically distinguished for sufficiently large $|z|$.

Schrödinger cat states are defined as

$$|\psi_{sc}\rangle = N_{sc}(|z\rangle + e^{i\phi}|-z\rangle), \tag{15}$$

where ϕ is the relative phase (can be taken on $[0, 2\pi]$) and N_{sc} is the normalization constant. For $\phi = 0$, we have the so-called even cat states, which exhibit vanishing odd number probability distribution $P_n^{(\mathrm{odd})} = |\langle n|\psi_{sc}\rangle|^2 = 0$. In contrast, for $\phi = \pi$, odd cat states that exhibit vanishing even number probability distribution $P_n^{(\mathrm{even})} = 0$ are obtained. This is one of the most interesting statistical behaviors of SCs and we examine the deformed GKSCs with these statistical properties in the subsequent sections.

With the same token, we can construct GKSCs. By letting $z = \sqrt{J}e^{-i\gamma}$, we have [49]

$$|\psi_{gksc}\rangle = N_{gksc}(|J,\gamma\rangle + e^{i\phi}|J,\gamma + \pi\rangle), \tag{16}$$

where we have denoted $|z\rangle = |J,\gamma\rangle$ and $|-z\rangle = |J,\gamma + \pi\rangle$. We further substitute (7) and obtain [49]

$$|\psi_{gksc}\rangle = N_{gksc} \sum_{n\geq 0}^{\infty} \left\{ \frac{J^{\frac{n}{2}} e^{-i\gamma\epsilon_n}}{\sqrt{\rho_n}} [1 + e^{i(\phi - \epsilon_n\pi)}] |n\rangle \right\}, \tag{17}$$

where $[N_{gksc}]^{-2} = 2\sum_{n\geq 0}^{\infty} (\frac{J^n}{\rho_n}[1 + \cos(\phi - \epsilon_n\pi)])$.

III. GKSCS WITH MINIMUM LENGTH AND/OR MAXIMUM MOMENTUM

Next, we introduce quantum deformation to Heisenberg algebra. Considering one dimension, such deformation can be generally expressed as following modified commutation relation (MCR)

$$[X,P] = i\hbar f(X,P), \tag{18}$$

where $f(X,P)$ captures the position and/or momentum dependence deformation and hence plays the crucial role in determining the modified dynamics. For $f(X,P)=1$, we recover the standard quantum mechanics. Different quantum deformation models are distinguished by the expression of $f(X,P)$ and this operator-valued function is essential to study different phenomenological effects of the deformation models. There are two important phenomenological models of quantum deformation in the literature, namely, the minimum length model, which is inspired by string theory, black hole physics, and loop quantum gravity, and the maximum momentum model, which is inspired by doubly special relativity. For a review on the generalized uncertainty principle induced by the modified commutation relation, see [23,24].

A. Deformation with minimal length

In the literature, one of the most interesting and nontrivial models to be considered is the Kempf-Mangano-Mann (KMM) model[10], which satisfies the relations[3]

$$[X,P] = i\hbar(1+\tilde{\beta}P^2); \qquad X = (1+\tilde{\beta}p^2)x, \qquad P = p \tag{19}$$

such that $\tilde{\beta} = \frac{\beta}{m\hbar\omega}$ with β being the dimensionless deformed parameter and $[\tilde{\beta}] = \text{momentum}^{-2}$. Here, both x and p are standard position and momentum operators that satisfy conventional commutation relation $[x,p] = i\hbar$. The modified relation exhibits an intrinsic minimum length as discussed in [102,103],

$$L_{\min} \coloneqq (\Delta X)|_{\min} \approx \hbar\sqrt{\tilde{\beta}}. \tag{20}$$

Next, we proceed to compute the deformed GKSCs for the case of minimum length. In order to do that, we need the quantum state and eigenenergy spectrum of the deformed one-dimensional simple harmonic oscillator. The perturbed Hamiltonian $H^{(ml)}$ of the deformed harmonic oscillator in noncommutative space is given by [69,72]

$$H^{(ml)} = \frac{P^2}{2m} + \frac{m\omega^2}{2}X^2 - \frac{\hbar\omega}{2}\left(1+\frac{\beta}{2}\right). \tag{21}$$

With representation of physical position operator X given in (19), the Hamiltonian (21) becomes non-Hermitian. Following [69,103], one can perform the Dyson map $\eta = (1+\tilde{\beta}p^2)^{-1/2}$, whose adjoint action relates the non-Hermitian Hamiltonian in (21) to its isospectral Hermitian counterpart $h^{(ml)}$,

$$\begin{aligned} h^{(ml)} &= \eta H^{(ml)}\eta^{-1} \\ &= \frac{p^2}{2m} + \frac{m\omega^2}{2}x^2 + \frac{\omega\beta}{4\hbar}[p^2x^2 + x^2p^2 + 2xp^2x \\ &\quad - 2i\hbar(xp+px)] - \frac{\hbar\omega}{2}\left(1+\frac{\beta}{2}\right) + O(\beta^2). \end{aligned} \tag{22}$$

The perturbed energy spectrum is given by

$$\frac{\epsilon_n^{(ml)}}{\hbar\omega} = n + \frac{n}{2}(n+1)\beta + O(\beta^2). \tag{23}$$

The term $O(\beta^2)$ can to be truncated from the phenomenological point of view. Notice that the deformed energy spectrum increases faster for higher n when compared to the standard case. The perturbed Hamiltonian eigenstates (up to first order in β) are given by the standard nondegenerate Rayleigh-Schrödinger perturbation theory,

$$\begin{aligned} |n\rangle_{ml} &= |n^{(0)}\rangle + \sum_{k\neq n}^{\infty}\frac{\langle k^{(0)}|h_1|n^{(0)}\rangle}{\epsilon_n^0 - \epsilon_k^0}|k^{(0)}\rangle \\ &= |n^{(0)}\rangle + \frac{\beta}{16}\left(\sqrt{\mathbf{P}[n+1,4]}|n^{(0)}+4\rangle \right. \\ &\quad \left. - \sqrt{\mathbf{P}[n-3,4]}|n^{(0)}-4\rangle\right), \end{aligned} \tag{24}$$

where $h_1 = \omega\beta(p^2x^2 + x^2p^2 + 2xp^2x - 2i\hbar(xp+px) - \hbar^2)/(4\hbar)$ is the perturbed Hamiltonian. We denoted $|n\rangle_{ml}$ and $|n^{(0)}\rangle$ as the perturbed and unperturbed Fock's state, respectively. Also, $\mathbf{P}[a,n] \equiv (a)_n$ is the Pochhammer symbol, which is a compact way to express the factorial,

$$\mathbf{P}[a,n] \equiv (a)_n \coloneqq \frac{(a+n-1)!}{(a-1)!}; \qquad (a)_0 \coloneqq 1. \tag{25}$$

It is clear that up to leading order in β, the perturbed eigenstates $|n\rangle_{ml}$ are not normalized in the usual manner because

$$\begin{aligned} {}_{ml}\langle m|n\rangle_{ml} &= \delta_{mn} + \frac{\beta}{16}\{(n+1)_4\delta_{m,n+4} \\ &\quad - (n-3)_4\delta_{m,n-4} + \text{terms } m \leftrightarrow n\}. \end{aligned} \tag{26}$$

Next, following [104] we can renormalize the perturbed Fock's state such that $\langle\xi_m^{(ml)}|\xi_n^{(ml)}\rangle = \delta_{mn}$ by defining

[3]The KMM model can be regarded as the three-dimensional realization of Snyder model [9], which was the first attempt to study Lorentz invariant discrete space-time back in the 1940s.

$$|\xi_n^{(ml)}\rangle := \sqrt{Z_n^{(ml)}}|n\rangle_{ml}. \tag{27}$$

The constant $Z_n^{(ml)}$ satisfies $Z_n^{(ml)} = |\langle n^{(0)}|\xi_n^{(ml)}\rangle|^2$ and thus can be regarded as the probability for the perturbed eigenstates to be found in the corresponding unperturbed eigenstate. Explicitly, it can be written as

$$Z_n^{(ml)} \approx 1 - \sum_{k\neq n}^{\infty} \frac{|\langle k^{(0)}|h_1|n^{(0)}\rangle|^2}{(\epsilon_n^0 - \epsilon_k^0)^2}. \tag{28}$$

Following the GK approach in Sec. II A, the KMM-deformed GKSCs are constructed as

$$|\psi_{gksc}^{(ml)}\rangle := N_{gksc}^{(ml)} \sum_{n\geq 0}^{\infty} \left\{ \frac{J_{\frac{n}{2}} e^{-i\gamma\epsilon_n^{(ml)}}}{\sqrt{\rho_n^{(ml)}}} [1 + e^{i(\phi - \epsilon_n^{(ml)}\pi)}] |\xi_n^{(ml)}\rangle \right\}, \tag{29}$$

with

$$\begin{aligned}\rho_n^{(ml)} &:= \prod_{k\geq 1}^{n} \epsilon_k^{(ml)} = \prod_{k\geq 1}^{n} \left[k + \frac{k(k+1)\beta}{2}\right] \\ &= \frac{1}{2^n}\beta^n n! \mathbf{P}[2 + 2/\beta, n],\end{aligned} \tag{30}$$

where $N_{gksc}^{(ml)}$ denotes the overall normalization constant and $\rho_n^{(ml)}$ is the probability distribution. Note that for the undeformed case $\beta = 0$, we have the Poisson distribution, $\rho_n = n!$.

B. Deformation with maximum momentum

Next, we consider another modified commutation relation that exhibits an intrinsic maximum momentum and is particularly favored by doubly special relativity [25–28] and the anti-Snyder model [33,105]. One such model is the Ali-Das-Vagenas (ADV) model [29,38]. In one dimension, it is described by the following MCR,

$$[X, P] = i\hbar(1 - \tilde{\alpha}P)^2; \quad X = x, \quad P = \frac{p}{1 + \tilde{\alpha}p}, \tag{31}$$

where $\tilde{\alpha} = \frac{\alpha_0}{M_{pl}c} = \frac{\alpha_0 L_{pl}}{\hbar}$, such that M_{pl} is the Planck mass while L_{pl} is the Plank length with $[\tilde{\alpha}^2] = [\tilde{\beta}] =$ momentum^{-2}. Also, α_0 is a dimensionless constant, typically assumed to be unity [29]. The above MCR manifestly exhibits an intrinsic maximum momentum

$$P_{\max} \approx \frac{1}{\tilde{\alpha}} \tag{32}$$

and the form of (31) suggests that one recovers the classicality around the maximum momentum [38].

The rescaled energy spectrum for the ADV deformed harmonic oscillator is given by

$$\begin{aligned}\frac{\epsilon_n^{(mm)}}{\hbar\omega} &= \frac{2n[4 + n\alpha^2\sqrt{2(2+\alpha^4)} - (n-1)\alpha^4]}{(\alpha^2 + \sqrt{2(2+\alpha^4)})[(2n+1)\alpha^2 + \sqrt{2(2+\alpha^4)}]^2} \\ &= n - \frac{3n}{2}(n+1)\alpha^2 + O(\alpha^4),\end{aligned} \tag{33}$$

where $\alpha = \sqrt{m\hbar\omega}\tilde{\alpha}$ is the dimensionless deformation parameter. Comparing (33) to the KMM model (23), the ADV-deformed bound state energy spectrum has a negative energy correction. This is the essential difference between these two models and it should be generic to all quantum mechanical bounded systems.

The (un-normalized) perturbed ADV-deformed Hamiltonian eigenstates (up to first order in α) are given by

$$\begin{aligned}|n\rangle_{mm} = |n^{(0)}\rangle - \frac{i\alpha}{3\sqrt{8}}\Big[&\sqrt{\mathbf{P}[n+1,3]}|n^{(0)}+3\rangle \\ &+ \sqrt{\mathbf{P}[n-2,3]}|n^{(0)}-3\rangle \\ &- 9((n+1)^{3/2}|n^{(0)}+1\rangle + n^{3/2}|n^{(0)}-1\rangle)\Big]\end{aligned} \tag{34}$$

and we can obtain the renormalized perturbed state as $\langle\xi_m^{(mm)}|\xi_n^{(mm)}\rangle = \delta_{mn}$ through the definition $|\xi_n^{(mm)}\rangle := \sqrt{Z_n^{(mm)}}|n\rangle_{mm}$. It follows that the ADV-deformed GKSCs can be constructed as

$$|\psi_{gksc}^{(mm)}\rangle := N_{gksc}^{(mm)} \sum_{n\geq 0}^{\infty} \left\{ \frac{J_{\frac{n}{2}} e^{-i\gamma\epsilon_n^{(mm)}}}{\sqrt{\rho_n^{(mm)}}} [1 + e^{i(\phi - \epsilon_n^{(mm)}\pi)}] |\xi_n^{(mm)}\rangle \right\} \tag{35}$$

with

$$\rho_n^{(mm)} := \prod_{k\geq 1}^{n} \epsilon_k^{(mm)} = \frac{n!(2\mu-1)^n \mathbf{P}[2(\mu+1), n]}{(2\alpha^2)^n (2\mu+1)^n (\mathbf{P}[\mu + \frac{3}{2}, n])^2}, \tag{36}$$

where we denote $\mu = \sqrt{\frac{1}{2} + \frac{1}{\alpha^4}}$ and $N_{gksc}^{(mm)}$ is the overall normalization constant. Also, note that for $\rho_n^{(mm)}|_{\alpha\to 0} = n!$ we recover the Poisson distribution.

IV. PROBABILITY DISTRIBUTION AND ENTROPY OF THE DEFORMED GKSCS

A. Normalization constant

To ensure the orthonormality condition $|\langle\psi_{gksc}^{(ml)}|\psi_{gksc}^{(ml)}\rangle|^2 = 1 = |\langle\psi_{gksc}^{(mm)}|\psi_{gksc}^{(mm)}\rangle|^2$ of the deformed GKSCs (29) and (35) the normalization constant $N(J)$ is fixed as follows. The normalization constant for KMM model is given by

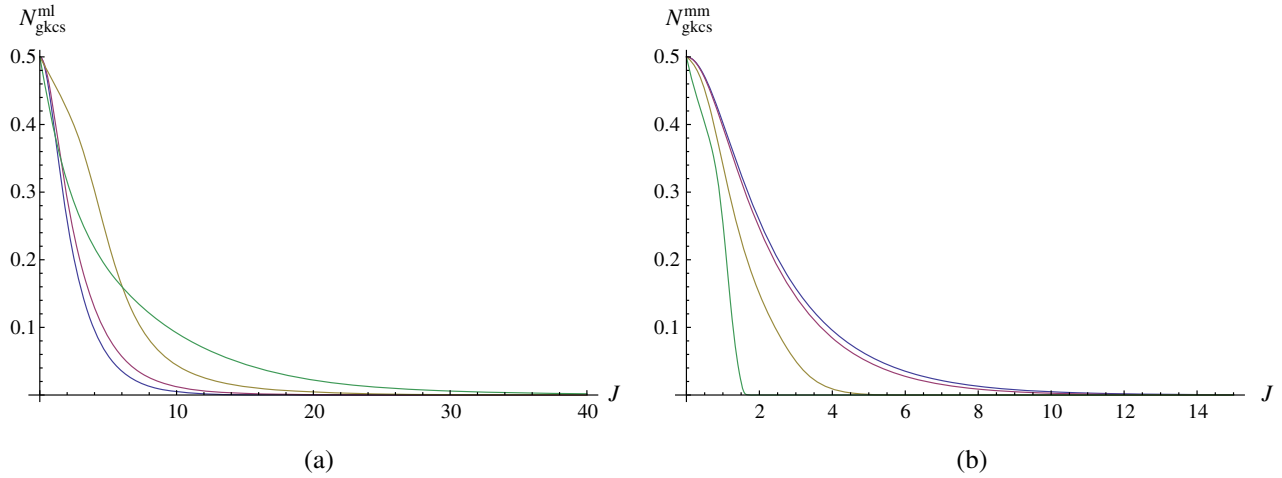

FIG. 1. The normalization constant N_{gksc} for both deformation cases with $\phi = 0$ (even cat states). The blue line corresponds to the undeformed case. (a) $N^{(ml)}_{gksc}$ for the minimum length (KMM) model corresponding to different values of deformed parameter β. Purple, gold and green lines are the deformed cases with $\beta = (0.1, 0.3, 0.7)$ respectively. (b) $N^{(mm)}_{gksc}$ for the maximum momentum (ADV) model corresponding to different values of deformed parameter α. Purple, gold and green lines are the deformed cases with $\alpha = (0.1, 0.3, 0.5)$ respectively.

$$N^{(ml)}_{gksc}(J,\beta,\phi) = \left(2\sum_{n=0}^{\infty}\frac{2^n J^n}{\beta^n n!\mathbf{P}[2+2/\beta,n]}[1+\cos(\phi-\epsilon_n^{(ml)}\pi)]\right)^{-1/2} \tag{37}$$

and for the ADV model is

$$N^{(mm)}_{gksc}(J,\alpha,\phi) = \left(2\sum_{n=0}^{\infty}\frac{2^n J^n \mathbf{P}[\mu+3/2,n]}{n!\alpha^{2n}\mathbf{P}[2(\mu+1),n]}[1+\cos(\phi-\epsilon_n^{(mm)}\pi)]\right)^{-1/2}. \tag{38}$$

In Fig. 1, we plot both $N^{(ml)}_{gksc}$ and $N^{(mm)}_{gksc}$ for even GKSCs ($\phi = 0$) as the function of average energy J for different values of deformation parameter β and α. As an approximation, we truncate the summation at $n = 100$ for KMM models and $n = 120$ for the ADV model. In both cases, we recover the undeformed normalization constant $N_{gksc}(J,\phi) = (2(e^J + e^{-J}\cos\phi))^{-1/2}$ as $(\beta,\alpha) \to 0$. In the KMM model, it is observed that $N^{(ml)}_{gksc}$ tends to increase with increasing β. In contrast, $N^{(mm)}_{gksc}$ in the ADV model tends to decrease with increasing α. Note that from the phenomenological point of view, the physically acceptable range of deformed parameter should be very small, $|\beta|, |\alpha| \ll 1$.

B. Probability distribution

It is well known that SCs have very specific statistical characteristics. In standard quantum optics, the even SCs ($\phi = 0$) have vanishing probability of detecting an odd number of photons while the odd SCs ($\phi = \pi$) have vanishing probability of detecting an even number of photons. It is interesting to find out whether the deformed GKSCs still possess these important statistical features. The probability distribution is defined as

$$P_n(J,\phi) \coloneqq |\langle n|\psi_{sc}\rangle|^2. \tag{39}$$

For the KMM model, the probability distribution is given by

$$P^{(ml)}_n(J,\phi,\beta) = |\langle\xi^{(ml)}_n|\psi^{(ml)}_{gksc}\rangle|^2 = 2(N^{(ml)}_{gksc})^2\frac{(2J)^n}{\beta^n n!\mathbf{P}[2+2/\beta,n]}[1+\cos(\phi-\epsilon_n^{(ml)}\pi)] \tag{40}$$

and we plot the probability distribution function as a function of J and n, respectively. For the even (odd) states, we set $\phi = 0$ ($\phi = \pi$).

From Figs. 2(a) and 3(a), we observed that KMM-deformed GKSCs do not possess the statistical characteristics of even (odd) SCs anymore. In Fig. 2(a), by setting $J = 20$, we notice that the even deformed GKSCs now possess nonvanishing odd probability distribution. Similarly, in Fig. 3(a), the odd deformed GKSCs possess nonvanishing even probability distribution. Consider the even deformed GKSCs; when the deformation parameter β increases, the probability of observing even n numbers of photons decreases and the peak is shifted towards smaller effective n. In contrast, the probability of observing odd n

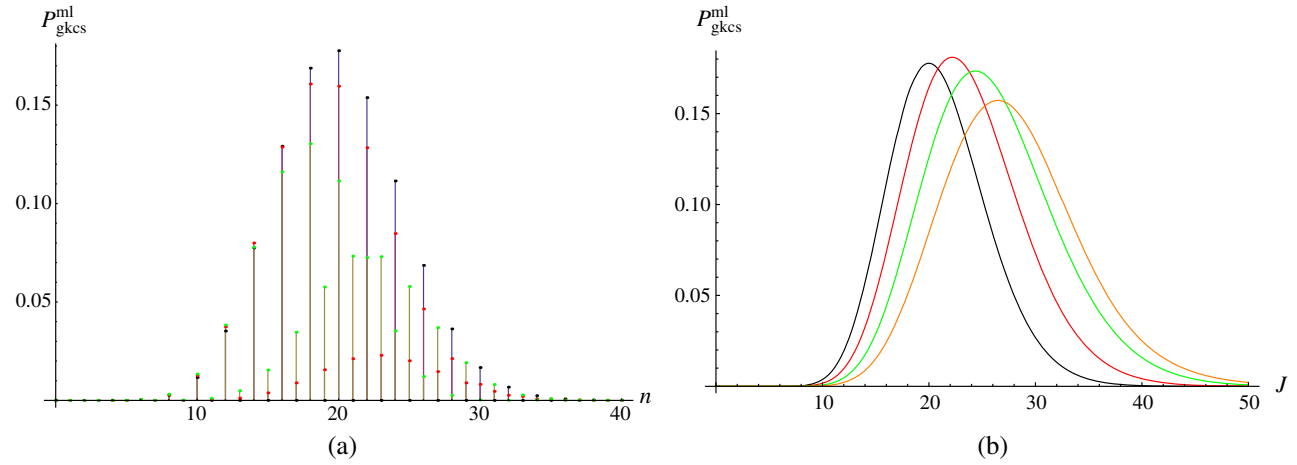

FIG. 2. The probability distribution $P_n^{(ml)}(J,\phi,\beta)$ for the minimum length (KMM) model with $\phi = 0$ corresponding to different values of deformation parameter β. (a) $P_n^{(ml)}(J,0,\beta)$ as function of n for $J = 20$. Black dot is the undeformed case while red and green dots are the deformed cases with $\beta = (0.001, 0.002)$ respectively. (b) $P_n^{(ml)}(J,0,\beta)$ as function of J for $n = 20$. Black line is the undeformed case while red, green and orange lines are the deformed cases with $\beta = (0.001, 0.002, 0.003)$ respectively.

numbers of photon, which is supposedly 0 in standard SCs, increases due to the deformation. A similar conclusion can be drawn on the odd deformed GKSC in Fig. 3(a). As a result, for a nonzero deformation β, it induces a mixture of two probability distributions to detect odd and even GKSCs, respectively. Effectively, this behavior shows up in a Kerr-type oscillator in nonlinear medium [49].

Next, we set the photon number $n = 20$ (even) and illustrate the probability distribution of even/odd KMM-deformed GKSCs in Figs. 2(b) and 3(b), respectively, corresponding to different values of β. It is observed that in Figs. 2(b) and 3(b), as the deformation increases, the probability decreases (increases) and spreads with the peak moving towards larger J. This can be understood from (23), such that the deformed energy spectrum increases with increasing deformation. We expect the average energy to increase and thus the peak of probability distribution shifts towards larger n.

For the ADV model with maximum momentum, we compute the probability distribution to be

$$\begin{aligned} P_n^{(mm)}(J,\phi,\alpha) &= |\langle \xi_n^{(mm)} | \psi_{gksc}^{(mm)} \rangle|^2 \\ &= 2(N_{gksc}^{(mm)})^2 \frac{[2J\alpha^2(2\mu+1)]^n (\mathbf{P}[\mu+3/2,n])^2}{n!(2\mu-1)^n \mathbf{P}[2(\mu+1),n]} \\ &\quad \times [1+\cos(\phi-\epsilon_n^{(mm)}\pi)]. \end{aligned} \tag{41}$$

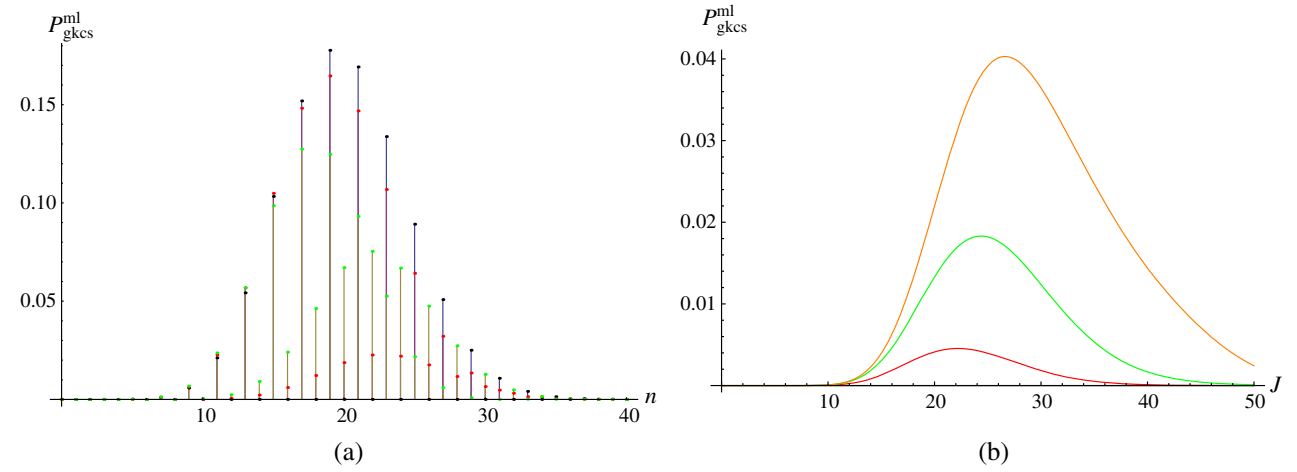

FIG. 3. The probability distribution $P_n^{(ml)}(J,\phi,\beta)$ for the minimum length (KMM) model with $\phi = \pi$ corresponding to different values of deformation parameter β. (a) $P_n^{(ml)}(J,\pi,\beta)$ as function of n for $J = 20$. Black dot is the undeformed case while red and green dots are the deformed cases with $\beta = (0.001, 0.002)$ respectively. (b) $P_n^{(ml)}(J,\pi,\beta)$ as function of J for $n = 20$. Black line is the undeformed case while red, green and orange lines are the deformed cases with $\beta = (0.001, 0.002, 0.003)$ respectively.

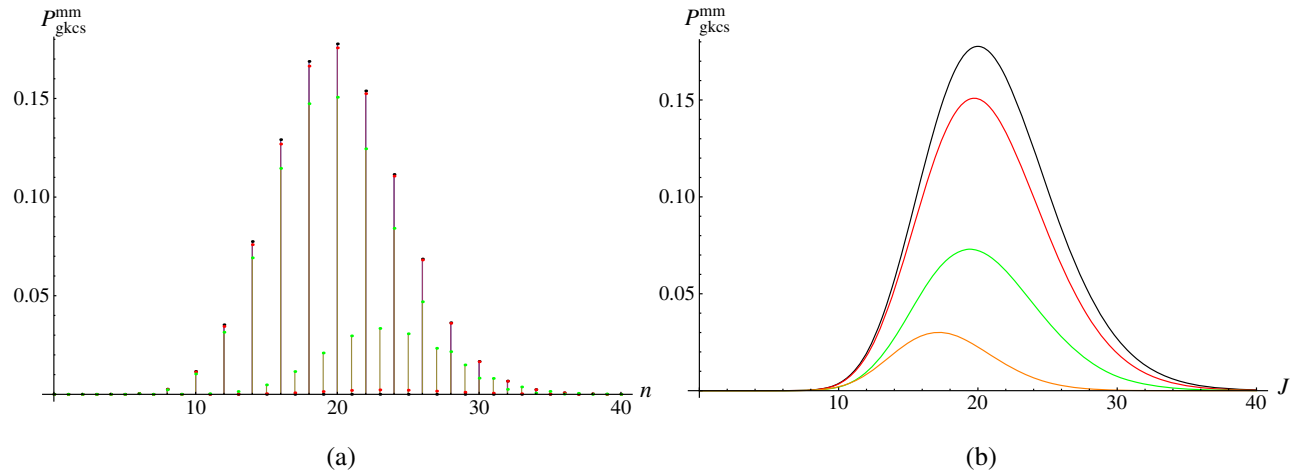

FIG. 4. The probability distribution $P_n^{(mm)}(J,\phi,\alpha)$ for the intrinsic maximum momentum (ADV) model with $\phi = 0$ corresponding to different values of deformed parameter α. (a) $P_n^{(mm)}(J,0,\alpha)$ as function of n for $J = 20$. Black dot is the undeformed case while red and green dots are the deformed cases with $\alpha = (0.01, 0.02)$ respectively. (b) $P_n^{(mm)}(J,0,\alpha)$ as function of J for $n = 20$. Black line is the undeformed case while red, green and orange lines are the deformed cases with $\alpha = (0.02, 0.03, 0.07)$ respectively.

Similar to the KMM model, we plot the probability distribution function as a function of n and J in the following graphs for even ($\phi = 0$) and odd ($\phi = \pi$) states separately.

From Figs. 4(a) and 5(a), we also observe that the ADV-deformed GKSCs do not possess even and odd statis tical characteristics. Similar to the KMM model, the even ADV-deformed GKSCs now possess relatively small but nonvanishing odd probability distribution while the odd ADV-deformed GKSCs possess small, nonvanishing even probability distribution. By setting the photon number to be $n = 20$, we illustrate the probability distribution of the even and odd ADV-deformed GKSCs as a function of energy J in Figs. 4(b) and 5(b) respectively. It is observed that in Fig. 4(b) as the deformation increases, the probability decreases and spreads with the peak moving towards smaller J. Figure 5(b) for the odd states shows contrasting trends. From (33), we see that the deformed energy spectrum decreases with increasing deformation. We expect the average energy to decrease and thus the peak of probability distribution to shift towards smaller n. This is the crucial difference between the KMM model and the ADV model as pointed out in [38].

In conclusion, we see that both KMM and ADV-deformed GKSCs generally do not possess the specific statistical features of standard SCs. However, some new

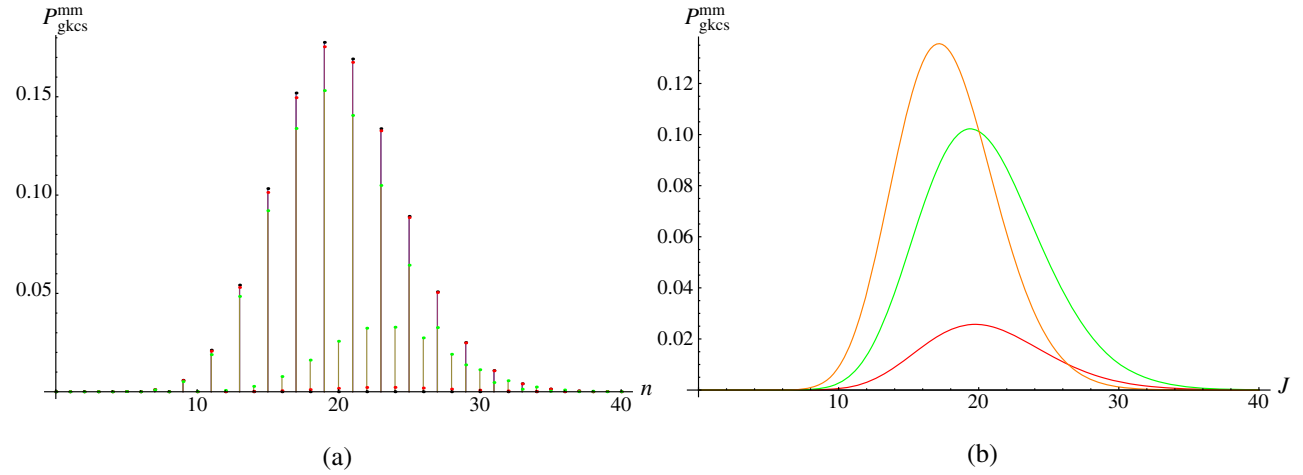

FIG. 5. The probability distribution $P_n^{(mm)}(J,\phi,\alpha)$ for the intrinsic maximum momentum (ADV) case with $\phi = \pi$ corresponding to different values of deformed parameter α. (a) $P_n^{(mm)}(J,\pi,\alpha)$ as function of n for $J = 20$. Black dot is the undeformed case while red and green dots are the deformed cases with $\alpha = (0.01, 0.02)$ respectively. (b) $P_n^{(mm)}(J,\pi,\alpha)$ as function of J for $n = 20$. Black line is the undeformed case while red, green and orange lines are the deformed cases with $\alpha = (0.02, 0.03, 0.07)$ respectively.

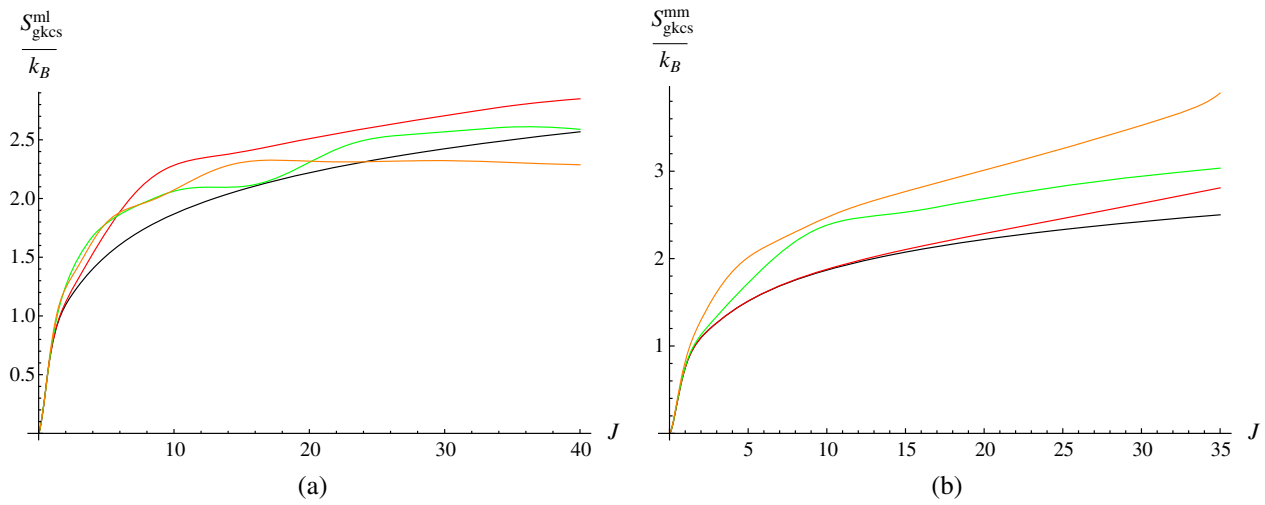

FIG. 6. Gibb's entropy for even GKSCs. (a) The entropy $S^{(ml)}$ for the KMM model with $\phi = 0$ corresponding to different values of deformed parameter β. Black line is the undeformed case while red, green and orange lines are the deformed cases with $\beta = (0.01, 0.05, 0.1)$ respectively. (b) The entropy $S^{(mm)}$ for the ADV model with $\phi = 0$ corresponding to different values of deformed parameter α. Black line is the undeformed case while red, green and orange lines are the deformed cases with $\alpha = (0.01, 0.05, 0.1)$ respectively.

statistical features may appear in the deformed GKSCs. Although in general the probability distribution is nonvanishing for deformed GKSCs, we see that from (40) and (41) it is possible for the term $[1 + \cos(\phi - \epsilon_n\pi)]$ to vanish for a certain state n and certain value of deformation parameter if $\phi - \epsilon_n\pi = (2\kappa + 1)\pi$ where $k \in Z$. This new feature can be useful in the study of the deviation in the photon's full counting statistics and Fanos noise factor that is induced by different classes of MCR. In principle, these two important classes of MCR can be distinguished by quantum optical experiment in the laboratory setting.

C. Entropy of KMM-/ADV-deformed GKSCs

Following [106], we define the Gibbs entropy of the system (canonical ensemble) as the standard logarithmic measure of the density of states in the phase space given by

$$S(J, \phi) := -k_B \sum_{n=0}^{\infty} P_n(J, \phi) \ln P_n(J, \phi), \tag{42}$$

where k_B is the Boltzmanns constant. This allows us to define the entropy of KMM-/ADV-deformed GKSCs in a similar way.

We plot the entropy of both KMM model $S^{(ml)}$ and ADV model $S^{(mm)}$ for even GKSCs as the function of the average energy J in Figs. 6(a) and 6(b), respectively. We observe that in both models with small deformation parameters (phenomenologically preferred), the entropy of deformed GKSCs is generally increased when compared to the undeformed SCs. The difference in entropy between the two deformations is not significant for small deformation parameters and short range average energy J. Similar results can be obtained for the odd-GKSCs case.

V. NONCLASSICAL PROPERTIES OF THE DEFORMED GKSCS

A. Photon statistics and number squeezing of GKSCs

In quantum optics, the measure of deviation from the standard Poissonian distribution is given by the famous Mandel parameter defined by

$$Q := \frac{\langle J, \gamma | (\Delta N)^2 | J, \gamma \rangle}{\langle J, \gamma | N | J, \gamma \rangle} - 1 = \frac{\sum_{n=0}^{\infty} n^2 P_n - (\sum_{n=0}^{\infty} n P_n)^2}{\sum_{n=0}^{\infty} n P_n} - 1. \tag{43}$$

The value of the Q number defines the characteristics of the quantum statistical distribution. $Q = 0$ corresponds to the standard Poissonian (classical) distribution, e.g., coherent light. For $Q > 0$, it refers to the super-Poissonian, which corresponds to photon bunching statistics, e.g., thermal light. For $Q < 0$, it refers to the sub-Poissonian, which corresponds to photon antibunching statistics, e.g., squeezed coherent light. For standard SCs, it is a well-known fact that even (odd) cat states exhibit photon number bunching (antibunching), respectively. Subsequently we examine the deviation induced by the quantum deformation on this unique characteristic of the cat states. For both of our deformed KMM and ADV models, we define

$$Q_q(J, \phi, q) = \frac{\sum_{n=0}^{\infty} n^2 P_n^q - (\sum_{n=0}^{\infty} n P_n^q)^2}{\sum_{n=0}^{\infty} n P_n^q} - 1, \tag{44}$$

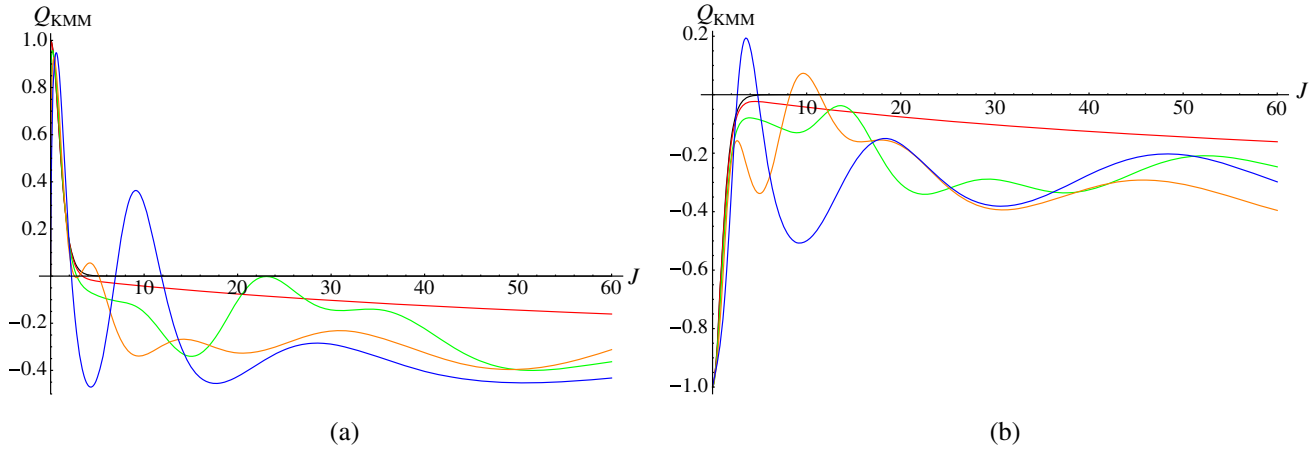

FIG. 7. Mandel parameter for KMM models Q_β with different values of deformation parameter β. The black line is the undeformed case while red, green, orange, and blue lines are the deformed cases with $\beta = (0.01, 0.05, 0.1, 0.15)$, respectively. (a) The Mandel parameter Q_β for the even GKSCs. (b) The Mandel parameter Q_β for the odd GKSCs.

where $q = (\beta, \alpha)$ refers to the classes of deformation, either KMM or ADV models, whereby the probability distributions are described by (40) and (41).

To obtain numerical plots, we perform suitable truncation up to $n = 400$ in the calculation of Q_β and Q_α, respectively.

In Figs. 7(a) and 7(b), we plot Mandel's parameter Q_β as a function of J for KMM even (odd) states, respectively. The illustrations show that the photon statistics of even (odd) KMM GKSCs can be super-/sub-Poissonian (positive/negative Q value) for small J, similar to the undeformed standard SCs. However, both even and odd cat states tend to become more nonclassical sub-Poissonian (negative Q value) as J increases. Note that the different amount of deformation β only affects the oscillatory behavior of Q_β but the Q values are always bounded to be negative for increasing J. Thus, in the KMM model, all the GKSCs get more nonclassical in the higher energy sector. Interestingly, the photon number distribution of the deformed even cat states experienced more squeezing compared to standard SCs, in which the latter is always photon-bunched $Q > 0$. However, for certain values of β and relatively small J, super-Poissionian is still possible.

In Figs. 8(a) and 8(b), we plot Mandel's parameter Q_α as a function of J for ADV GKSCs even (odd) states, respectively. For small J, both even (odd) states remained photon bunched (antibunched), similar to the undeformed case. However, as J increases, the Q_α values of even states still remain positive and increase with J and α while the odd states become super-Poissionian. Thus, all of the GKSCs get more classical for the ADV model in the higher energy sector. Note that from the phenomenological point of view, larger values of J should be physically more relevant.

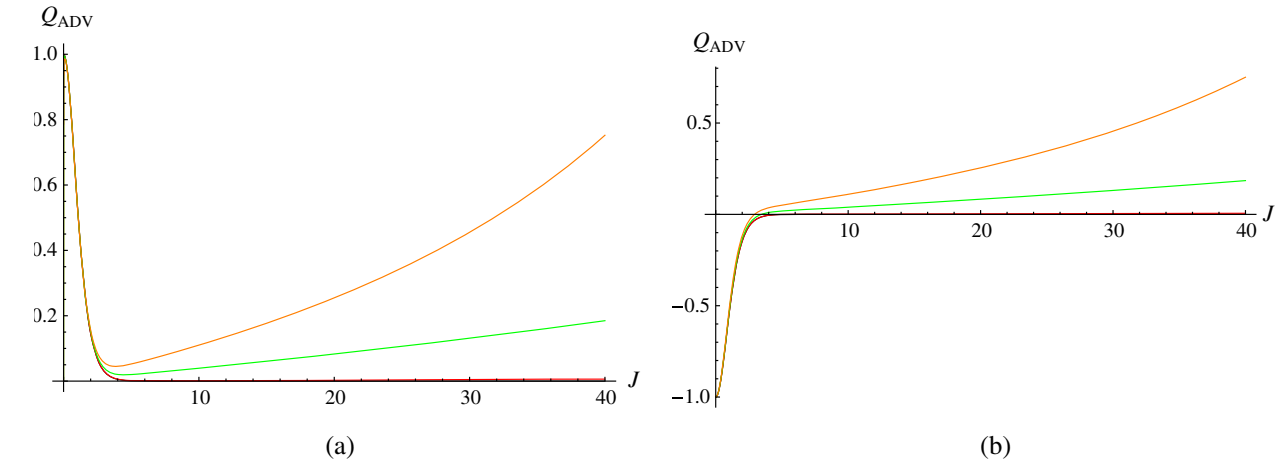

FIG. 8. Mandel parameter for ADV models Q_α with different values of deformation parameter α. The black line is the undeformed case while the red, green, and orange lines are the deformed cases with $\alpha = (0.01, 0.05, 0.08)$, respectively. (a) The Mandel parameter Q_α for the even GKSCs. (b) The Mandel parameter Q_α for the odd GKSCs.

The existence of such classicality is intimately related to the vanishing MCR in (31) as $P \to P_{\max} = \frac{1}{\hat{\alpha}}$.

In comparison between the two models, we realize that, in principle, we can distinguish both KMM (minimal length) and ADV (maximum momentum) MCR via Mandel's parameter since the former becomes more squeezed and exhibits sub-Poissonian distribution while the latter becomes more classical with super-Poissonian distribution. In [69], it was shown that for the deformed GK coherent states, the KMM model predicts gravitational squeezing with sub-Poissonian distribution regardless of deformation β and γ (action variable). Similar behavior is observed in our results on both KMM-even (odd) cat states. However,[48] showed that it is possible for ADV-deformed GK coherent states to exhibit both types of quantum statistics that depends on the γ factor. This generic behavior is different to the cat states counterpart in our ADV models.

B. Quadrature squeezing of GKSCs

Besides the number squeezing effect introduced by the deformation of the GKSCs, here we consider another famous quantum optical effect, namely, quadrature squeezing. Since the standard creation and annihilation operators ($A^\dagger$ and A) do not act as ladder operators in the new deformed Fock's space [107], we search for modified ladder operators $A_q^\dagger$ and A_q that act genuinely on the perturbed Hamiltonian eigenstates $|\xi_n^q\rangle$. The perturbative treatment is kept up to leading order in the deformation parameters. First, we define

$$A_q|\xi_n^q\rangle = \sqrt{n}|\xi_{n-1}^q\rangle; \qquad A_q^\dagger|\xi_n^q\rangle = \sqrt{n+1}|\xi_{n+1}^q\rangle;$$
$$N_q|\xi_n^q\rangle = n|\xi_n^q\rangle, \tag{45}$$

where $q = (\beta, \alpha)$ refers to the class of deformations. Also, the modified ladder operators are required to obey the usual relations, $N_q = A_q^\dagger A_q$; $A_q^\dagger = (A_q)^\dagger$; $[A_q, A_q^\dagger] = 1$. Consider the KMM model; by a direct calculation we have

$$\begin{aligned}
&(A_\beta - A)|\xi_n^{(ml)}\rangle \\
&= \sqrt{n}|\xi_{n-1}^{(ml)}\rangle - A|\xi_n^{(ml)}\rangle \\
&= \frac{\beta}{16}\{(\sqrt{n\mathbf{P}[n,4]} - \sqrt{(n+4)\mathbf{P}[n+1,4]})|n+3\rangle \\
&\quad + (\sqrt{(n-4)\mathbf{P}[n-3,4]} - \sqrt{n\mathbf{P}[n-4,4]})|n-5\rangle\} \\
&= -\frac{\beta}{4}(A^\dagger)^3|\xi_n^{(ml)}\rangle + O(\beta^2).
\end{aligned} \tag{46}$$

Thus, perturbatively up to leading order in β, the KMM-modified ladder operator is

$$A_\beta = A - \frac{\beta}{4}(A^\dagger)^3. \tag{47}$$

Similarly, for the ADV model we have

$$\begin{aligned}
&(A_\alpha - A)|\xi_n^{(mm)}\rangle \\
&= \sqrt{n}|\xi_{n-1}^{(mm)}\rangle - A|\xi_n^{(mm)}\rangle \\
&= \left[\frac{i\alpha}{\sqrt{8}}(A^\dagger)^2 - 3A^2 - 3(2N+1)\right]|\xi_n^{(mm)}\rangle + O(\alpha^2),
\end{aligned} \tag{48}$$

and the perturbative expansion for the ADV-modified ladder operator is given by

$$A_\alpha = A + \frac{i\alpha}{\sqrt{8}}(A^\dagger)^2 - 3A^2 - 3(2N+1), \tag{49}$$

where $N = A^\dagger A$ is the usual number operator.

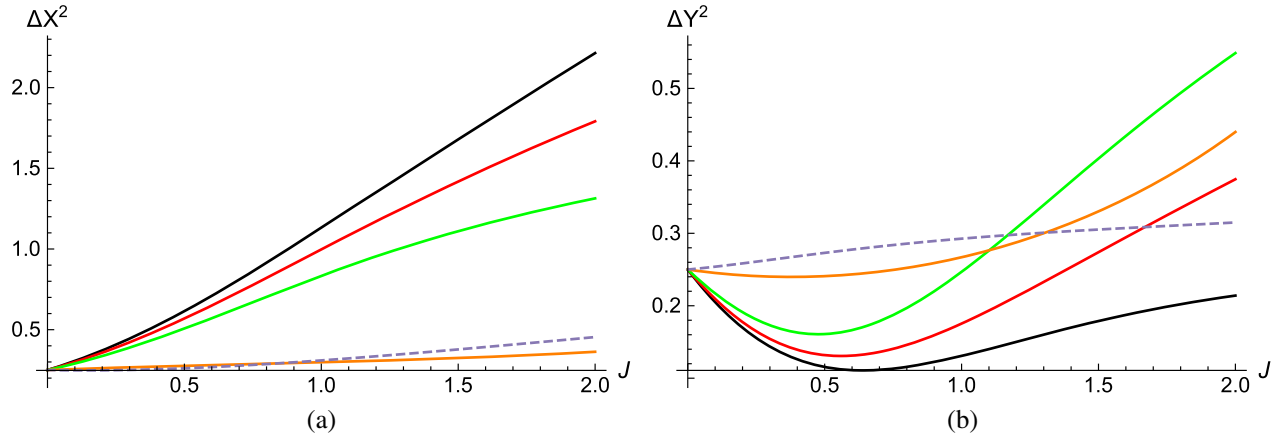

FIG. 9. The quadrature $(\Delta X_\beta)^2$ and $(\Delta Y_\beta)^2$ for the even GKSCs with different values of deformation parameter β. The black line is the undeformed case while the red, green, orange, and dashed lines are the deformed cases with $\beta = (0.05, 0.1, 0.3, 1.2)$, respectively. (a) Quadrature $(\Delta X_\beta)^2$ for the even GKSCs. (b) Quadrature $(\Delta Y_\beta)^2$ for the even GKSCs.

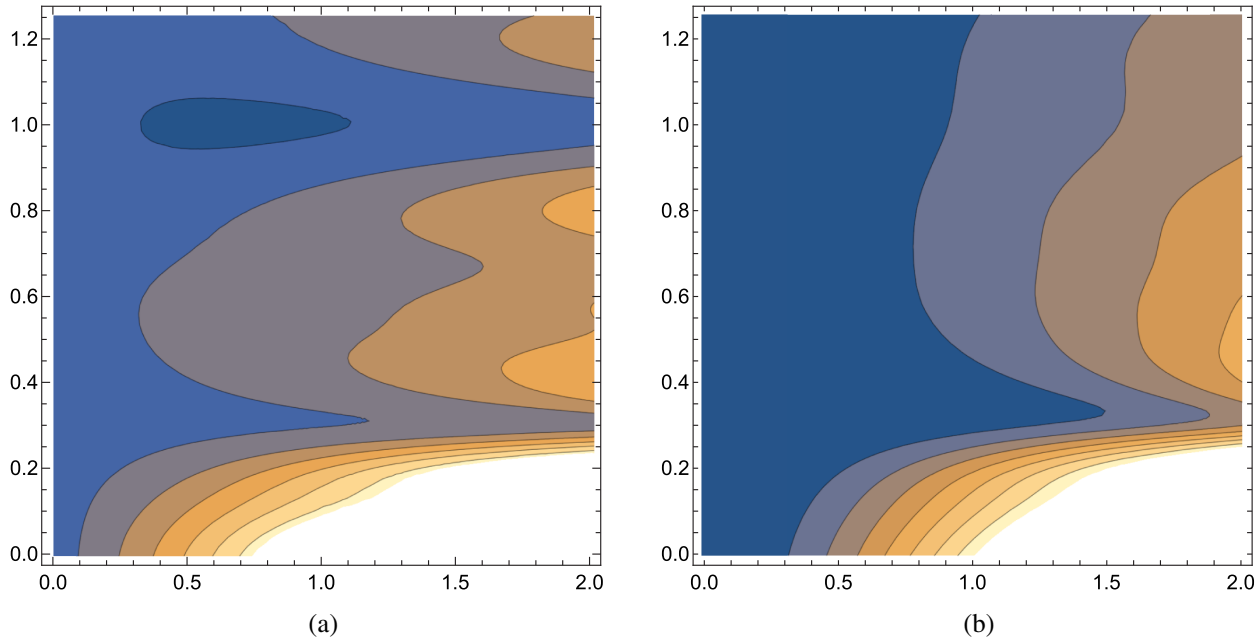

FIG. 10. Contour plot of the quantum noise as a function of J (horizontal axis) and deformation parameters β (vertical axis). Darker colors refer to smaller values. (a) Quantum noise $(\Delta X_\beta)^2$ for the even GKSCs as function of J and β. (b) Total quantum noise $T = (\Delta X_\beta)^2 + (\Delta Y_\beta)^2$ for the even GKSCs as function of J and β.

Next, we define the two quadrature operators as

$$X_q = \frac{1}{2}(A_q + A_q^\dagger); \qquad Y_q = \frac{1}{2i}(A_q - A_q^\dagger)$$
$$\Rightarrow X_q^2 = \frac{1}{4}(A_q^2 + (A_q^\dagger)^2 + 2N_q + 1);$$
$$Y_q^2 = -\frac{1}{4}(A_q^2 + (A_q^\dagger)^2 - 2N_q - 1), \tag{50}$$

and it is clear that X_q and Y_q are essentially dimensionless position and momentum operators

$$X = \sqrt{\frac{2\hbar}{m\omega}}X_q; \qquad P = \sqrt{2m\hbar\omega}Y_q.$$

The square of the uncertainties in state $|\psi_{gksc}\rangle_q$ is

$$(\Delta X_q)^2 = {}_q\langle\psi_{gksc}|X_q^2|\psi_{gksc}\rangle_q - {}_q\langle\psi_{gksc}|X_q|\psi_{gksc}\rangle_q^2, \tag{51}$$

$$(\Delta Y_q)^2 = {}_q\langle\psi_{gksc}|Y_q^2|\psi_{gksc}\rangle_q - {}_q\langle\psi_{gksc}|Y_q|\psi_{gksc}\rangle_q^2. \tag{52}$$

We plot the quadrature $(\Delta X_q)^2$ and $(\Delta Y_q)^2$ of even GKSCs for the KMM model (with various deformation parameters β) as a function of the average energy J in Figs. 9(a) and 9(b), respectively. The odd GKSCs generally produce similar trends. We see that unlike the coherent state, uncertainties in two quadratures in deformed GKSCs are not equal to each other. The quadrature $(\Delta X_\beta)^2$ is squeezed below the standard case, i.e., GKSCs ($\beta = 0$), whereas the quadrature $(\Delta Y_\beta)^2$ is expanded correspondingly. This means that we can reduce the quantum noise in the X_β variable. The condition eventually translates to more precise localization in position. Moreover, the total quantum noise $T := (\Delta X_q)^2 + (\Delta Y_q)^2$ also decreases when compared to the standard case. In Figs. 10(a) and 10(b), we plot the quantum noise in position $(\Delta X_\beta)^2$ and the total quantum noise T as a function of J and the deformation parameters β. We can adjust the values of J with varying deformation parameters β; we manage to obtain the so-called "ideal squeezed state," which is the minimum

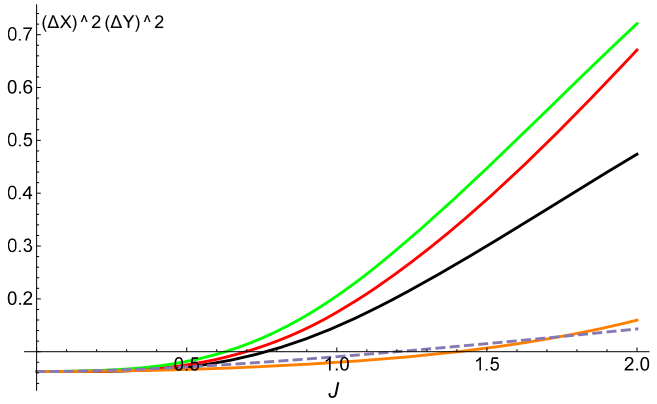

FIG. 11. Generalized uncertainty $(\Delta X_\beta)^2(\Delta Y_\beta)^2$ for the even GKSCs as a function of J with different values of deformation parameter β. The black line is the undeformed case while the red, green, orange, and dashed lines are the deformed cases with $\beta = (0.05, 0.1, 0.3, 1.2)$, respectively.

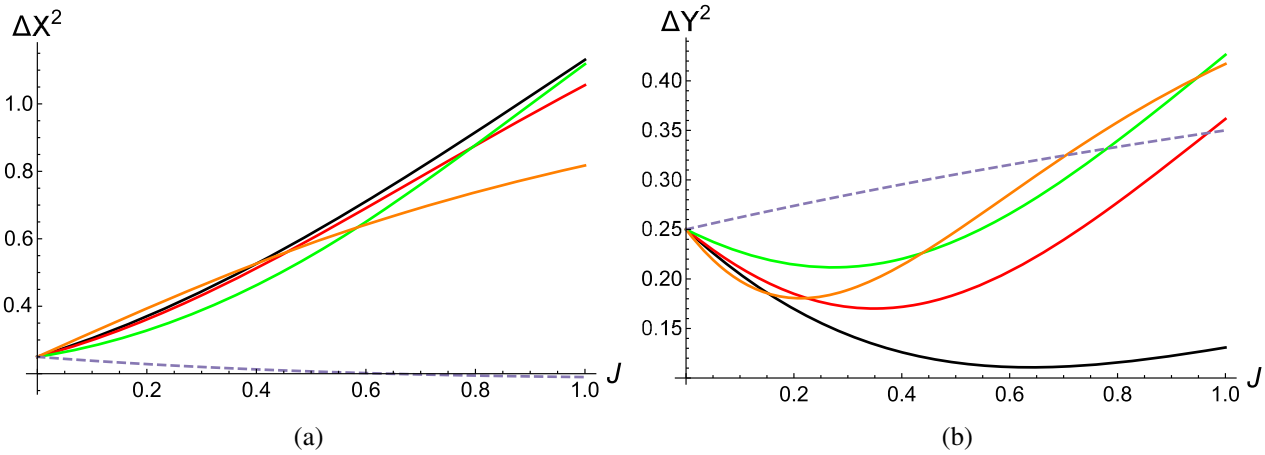

FIG. 12. The quadrature $(\Delta X_\alpha)^2$ and $(\Delta Y_\alpha)^2$ for the even GKSCs with different values of deformation parameter α. The black line is the undeformed case while the red, green, orange, and dashed lines are the deformed cases with $\alpha = (0.22, 0.35, 0.55, 1.00)$, respectively. (a) Quadrature $(\Delta X_\alpha)^2$ for the even GKSCs. (b) Quadrature $(\Delta Y_\alpha)^2$ for the even GKSCs.

uncertainty state with smallest squeezing in $(\Delta X_\beta)^2$. Numerically, we obtain such a state with $\beta = 1.00001$ and $J = 0.658773$. It is clearly shown in Fig. 10(a). Furthermore, interestingly we observe that for any fixed energy J, the total quantum noise T reduces for increasing β up to a certain threshold β_T and increases when $\beta > \beta_T$. At the same time, the total quantum noise is kept bounded from above by the standard ($\beta = 0$) reading as clearly shown in Fig. 10(b).

Next, we consider the generalized uncertainty of the quadrature pairs $(\Delta X_\beta)(\Delta Y_\beta)$. In Fig. 11, we see that there are constraints on both J and deformation parameters β in order to satisfy the inequality

$$(\Delta X_\beta) \cdot (\Delta Y_\beta) \geq (\Delta X_{\beta=0}) \cdot (\Delta Y_{\beta=0}). \tag{53}$$

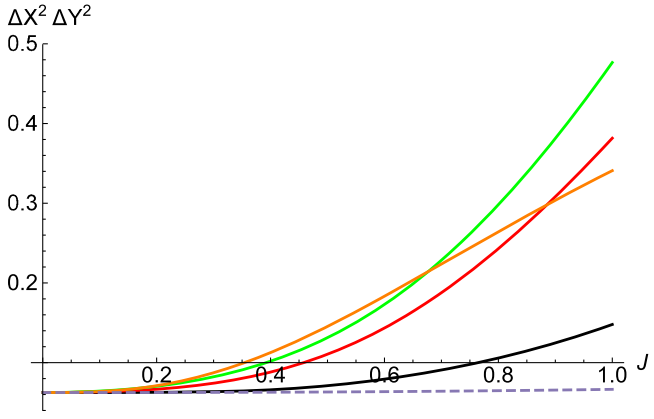

FIG. 13. Generalized uncertainty $(\Delta X_\alpha)^2(\Delta Y_\alpha)^2$ for the even GKSCs as a function of J with different values of deformation parameter α. The black line is the undeformed case while the red, green, orange, and dashed lines are the deformed cases with $\alpha = (0.22, 0.35, 0.55, 1.00)$, respectively.

From the form of MCR in (19), we do not expect KMM deformed GKSCs to approach classical phase (i.e., with vanishing GUP) and hence the inequality (53) has to be strictly satisfied. Numerically, deformation is meaningful if $\beta \leq \beta_{\max} \approx 0.23$ for the range of energy J we considered. However, in the higher energy sector that is physically more preferred from the phenomenological point of view, it remains possible to satisfy (53) with larger values of β. Similar results are obtained for the GKSCs odd state.

For the ADV model, we plot the quadrature $(\Delta X_\alpha)^2$ and $(\Delta Y_\alpha)^2$ of even GKSCs as the function of the average energy J in Figs. 12(a) and 12(b), respectively. Unlike the KMM model, deformed quantum noise in first quadrature $(\Delta X_\alpha)^2$ can be increased or decreased (depending on the range of energy J and the amount of deformation) as compared to the undeformed case. In contrast, $(\Delta X_\beta)^2$ always decreases while $(\Delta Y_\beta)^2$ always increases in the KMM model. We infer that improvement in spatial resolution and thus reduction of quantum noise is not

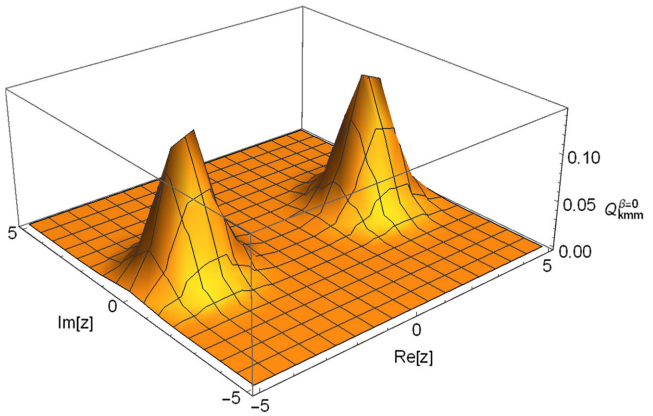

FIG. 14. The Husimi function $\mathcal{Q}(z)$ for the undeformed SCs case with $J = 10$, $\phi = 0 = \gamma$.

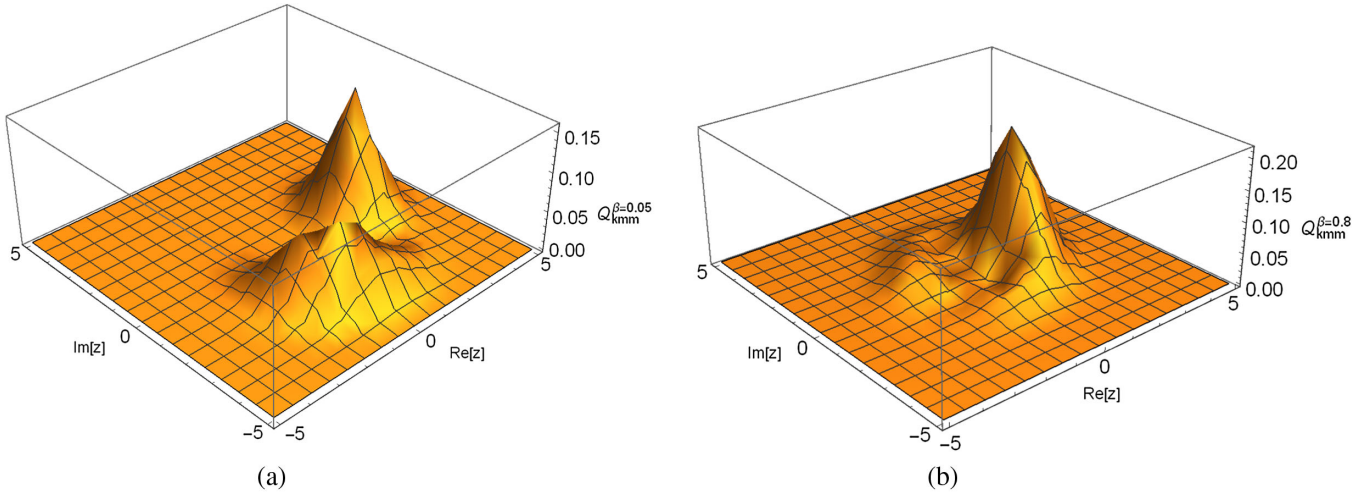

FIG. 15. The Husimi function $\mathcal{Q}(z)$ for the KMM-deformed GKSCs with different deformation β. (a) $\beta = 0.05$. (b) $\beta = 0.8$.

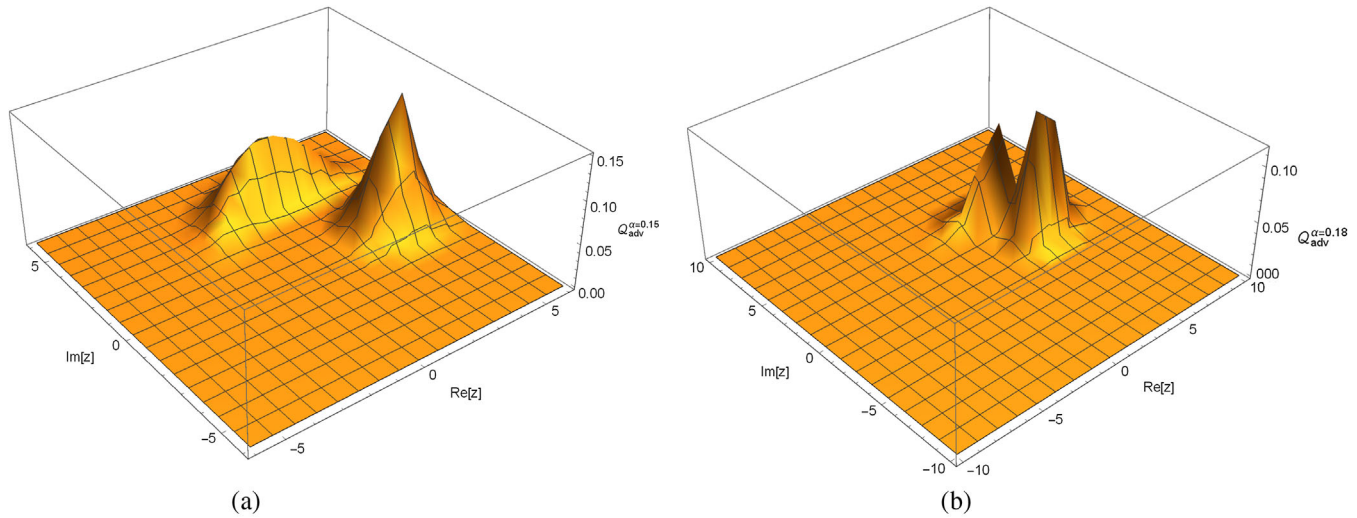

FIG. 16. The Husimi function $\mathcal{Q}(z)$ for the ADV-deformed GKSCs with different deformation α. (a) $\alpha = 0.15$. (b) $\alpha = 0.18$.

guaranteed for ADV-deformed GKSCs. Next, we consider the generalized uncertainty principle $(\Delta X_\alpha)(\Delta Y_\alpha)$ in Fig. 13. In contrast to the KMM model, we do not require the quadratures in the ADV model to strictly satisfy (53). From (31), we expect the emergence of classicality in the ADV model when the energy scale is approaching maximum momentum $P \to P_{\max} \approx \frac{1}{\alpha}$. In summary, we observed that the two classes of quantum deformation induce slight differences in their effects on the GKSCs.

VI. HUSIMI DISTRIBUTION

It is a well-known fact that SCs are formed by a superposition of two macroscopically distinguishable states; this was emphasized by Schrödinger himself in his original work. To study the superposition effect in deformed GKSCs, we consider the phase space distribution as a natural quantifier [49,55–57]. In the literature, there are two important probability distributions to characterize the phase space properties, the so-called Wigner $\mathcal{W}$ distribution and Husimi $\mathcal{Q}$ distribution. The Husimi distribution is given by the coherent state expectation value of the density operator or equivalently the overlap between the wave function and coherent state. It is strictly non-negative by construction. Here, we choose to explore the Husimi distribution[4] for the KMM/ADV-deformed GKSCs.

For the GKSCs, since the density of matrix is $\rho_q = |\psi_{gksc}\rangle_q \otimes {}_q\langle\psi_{gksc}|$, we define the corresponding Husimi $\mathcal{Q}$ function as

[4]Note that this choice would be clearly insufficient if we were interested in nonclassical properties indicated by the deformed GKSCs. Nonclassicality can be well understand in a negative value of the Wigner $\mathcal{W}$ function [49,108,109].

$$\mathcal{Q}(z) := \frac{1}{\pi}\langle z|\rho_q|z\rangle = \frac{1}{\pi}|\langle z|\psi_{gksc}\rangle_q|^2. \tag{54}$$

This definition ensures that the Husimi function is normalized $\int dz^2\mathcal{Q}(z) = 1$ and bounded $0 < \mathcal{Q}(z) < 1/\pi$. We have the explicit form in Fock's basis as

$$\mathcal{Q}(z) = \frac{1}{\pi}e^{-|z|^2}\sum_{n,m} C_n C_m^* \frac{z^m(z^*)^n}{\sqrt{n!m!}}, \tag{55}$$

where the constant C_n is

$$C_n = N^q_{gksc}\frac{J^{n/2}}{\sqrt{\rho^q_n}}e^{-i\epsilon^q_n\gamma}[1+\cos(\phi-\epsilon^q_n\pi)]. \tag{56}$$

By setting $J = 10$; $\phi = 0 = \gamma$, $q = 0$, we illustrate the Husimi distribution for even $\phi = 0$ standard GKSCs in the following figures. In Fig. 14, two sharp peaks corresponding to two coherent states in standard SCs are clearly shown for the underformed case.

For the KMM model, when the deformation parameter β increases, the well-localized catlike state gradually merges together and the two coherent states become indistinguishable. This is illustrated in Figs. 15(a) and 15(b).

For the ADV model, similar results are obtained as clearly shown in Figs. 16(a) and 16(b). Although the peaks are clearly observed for a small value of α, as α increases, the peaks become nonseparable. The result for odd cat states $\phi = \pi$ is essentially similar to the even cat states. We interpret this result as some kind of gravitational decoherence [110,111] due to minimal length/maximum momentum. In addition, for deformed GKSCs with "peaks merged" Husimi function, there does not seem to be an effective method to determine which form of the deformation the system undergoes.

VII. CONCLUSION

In this paper, we have successfully constructed deformed GKSCs under two important quantum gravity phenomenological models that exhibit minimal length scale (KMM model) and maximum momentum scale (ADV model). First, we review the generalized Heisenberg algebra scheme. This allows us to define the characteristic function and the weight function of the deformed GKCs. Formally, we can proceed to take the linear superposition of such states to obtain the deformed GKSCs.

We have computed the probability density and entropy distribution function in both models (for even and odd cat states) and subsequently studied their behavior in terms of the deformation parameters. Under finite deformation, even GKSCs possess small, nonvanishing odd probability distribution while odd GKSCs possess nonvanishing even probability distribution. We interpret this deviation from standard GKSCs as gravitational induced mixture of the two probability distributions to detect odd and even GKSCs, respectively. The entropy of the system increases in the presence of deformation. These observations are valid in both models and are insensitive to the type of deformation model.

To study the nonclassical behavior, we have considered number squeezing (defined in terms of Mandel's Q parameter) and quadrature squeezing. We realized that in principle we can distinguish both KMM and ADV model via Mandel's parameter since the former becomes more squeezed and exhibits sub-Poissonian distribution while the latter becomes more classical with super-Poissonian distribution. Furthermore, first quadrature squeezing ΔX_β in the KMM model always reduces with increasing deformation parameter β. This also means that KMM deformation leads to better spatial resolution and reduction of quantum noise. However, this desired behavior is not guaranteed in the ADV model since ΔX_α can be larger or smaller than the undeformed case. Lastly, we observed that the quantum coherency of deformed GKSCs is destroyed by the deformations as clearly shown in the indistinguishability of the peaks in the Husimi function $\mathcal{Q}(z)$.

ACKNOWLEDGMENTS

We thank the referee(s) for the valuable and critical comments for improvement of the presentation.

[1] J. Polchinski, *String Theory* (Cambridge University Press, Cambridge, England, 2005), Vol. 1 and 2.
[2] K. Becker, *String Theory and M-Theory: A Modern Introduction* (Cambridge University Press, Cambridge, England, 2007).
[3] C. Rovelli, Living Rev. Relativity **11**, 5 (2008).
[4] A. Ashtekar and J. Pullin, *loop quantum gravity: The First 30 Years* (World Scientific, Singapore, 2017).
[5] A. Connes, *noncommutative geometry* (Academic Press, Sand Diego, CA 1994).
[6] M. R. Douglas and N. A. Nekrasov, Rev. Mod. Phys. **73**, 977 (2001).
[7] M. Reuter and F. Saueressig, Phys. Rev. D **65**, 065016 (2002).
[8] R. J. Adler, Am. J. Phys. **78**, 925 (2010).
[9] H. S. Snyder, Phys. Rev. **71**, 38 (1947).

[10] A. Kempf, G. Mangano, and R. B. Mann, Phys. Rev. D **52**, 1108 (1995).
[11] A. Kempf, J. Phys. A **30**, 2093 (1997).
[12] L. N. Chang, D. Minic, N. Okamura, and T. Takeuchi, Phys. Rev. D **65**, 125028 (2002).
[13] Z. Lewis and T. Takeuchi, Phys. Rev. D **84**, 105029 (2011).
[14] L. N. Chang, Z. Lewis, D. Minic, and T. Takeuchi, Adv. High Energy Phys. **2011**, 493514 (2011).
[15] C. Quesne and V. M. Tkachuk, Phys. Rev. A **81**, 012106 (2010).
[16] F. Brau, J. Phys. A **32**, 7691 (1999).
[17] U. Harbach, S. Hossenfelder, M. Bleicher, and H. Stocker, Phys. Lett. B **584**, 109 (2004).
[18] S. Das and E. C. Vagenas, Phys. Rev. Lett. **101**, 221301 (2008).
[19] K. Nozari and P. Pedram, Europhys. Lett. **92**, 50013 (2010).
[20] D. Bouaziz and N. Ferkous, Phys. Rev. A **82**, 022105 (2010).
[21] M. Kober, Phys. Rev. D **82**, 085017 (2010).
[22] P. Pedram, J. Phys. A **45**, 505304 (2012).
[23] S. Hossenfelder, Living Rev. Relativity **16**, 2 (2013).
[24] A. N. Tawfik and A. M. Diab, Rep. Prog. Phys., **78**, 126001 (2015).
[25] J. Magueijo and L. Smolin, Phys. Rev. Lett. **88**, 190403 (2002).
[26] J. Magueijo and L. Smolin, Phys. Rev. D **67**, 044017 (2003).
[27] J. L. Cortes and J. Gamboa, Phys. Rev. D **71**, 065015 (2005).
[28] G. Amelino-Camelia, Phys. Lett. B **510**, 255 (2001).
[29] A. F. Ali, S. Das, and E. C. Vagenas, Phys. Lett. B **678**, 497 (2009).
[30] A. F. Ali, S. Das, and E. C. Vagenas, Phys. Rev. D **84**, 044013 (2011).
[31] S. Das, E. C. Vagenas, and A. F. Ali, Phys. Lett. B **690**, 407 (2010).
[32] P. Pedram, Phys. Lett. B **702**, 295 (2011).
[33] S. Mignemi, Phys. Rev. D **84**, 025021 (2011).
[34] P. Jizba, H. Kleinert, and F. Scardigli, Phys. Rev. D **81**, 084030 (2010).
[35] M. Maggiore, Phys. Lett. B **319**, 83 (1993).
[36] M. V. Battisti, Phys. Rev. D **79**, 083506 (2009).
[37] P. Pedram, Phys. Lett. B **714**, 317 (2012); **718**, 638 (2012).
[38] C. L. Ching, R. Parwani, and K. Singh, Phys. Rev. D **86**, 084053 (2012).
[39] G. Amelino-Camelia, Int. J. Mod. Phys. D **11**, 35 (2002); **11**, 1643 (2002).
[40] J. Magueijo and L. Smolin, Phys. Rev. Lett. **88**, 190403 (2002).
[41] I. Pikovski, M. R. Vanner, M. Aspelmeyer, M. Kim, and C. Brukner, Nat. Phys. **8**, 393 (2012).
[42] F. Marin, F. Marino *et al.*, Nat. Phys. **9**, 71 (2013).
[43] M. Bawaj, C. Biancofiore *et al.*, Nat. Commun. **6**, 7503 (2015).
[44] D. Gao and M. Zhan, Phys. Rev. A **94**, 013607 (2016).
[45] M. A. C. Rossi, T. Giani, and M. G. A Paris, Phys. Rev. D **94**, 024014 (2016).
[46] S. Dey, A. Bhat, D. Momeni, M. Faizal, A. F. Ali, T. K. Dey, and A. Rehman, Nucl. Phys. **B924**, 578 (2017).
[47] R. Howl, L. Hackermller, D. E. Bruschi, and I. Fuentes, Adv. Phys. X **3**, 1383184 (2018).
[48] C. L. Ching and W. K. Ng, Phys. Rev. D **88**, 084009 (2013).
[49] J. Dajka and J. Luczka, J. Phys. A **45**, 244006 (2012).
[50] J. R. Klauder, Ann. Phys. (N.Y.) **11**, 123 (1960).
[51] J. R. Klauder, J. Math. Phys. (N.Y.) **4**, 1055 (1963).
[52] R. J. Glauber, Phys. Rev. Lett. **10**, 84 (1963).
[53] E. C. G. Sudarshan, Phys. Rev. Lett. **10**, 277 (1963).
[54] J. P. Gazeau, *Coherent states in Quantum Physics* (Wiley Press, Berlin, 2009).
[55] J. R. Klauder and B. S. Skagertan, *Coherent states: Applications in Physics and Mathematical Physics* (World Scientific, Singapore, 1985).
[56] M. O. Scully and M. S. Zubairy, *Quantum Optics* (Cambridge University Press, Cambridge, England, 1997).
[57] L. Mandel and E. Wolf, *Optical Coherence and Quantum Optics* (Cambridge University Press, Cambridge, England, 1995).
[58] D. F. Walls, Nature (London) **306**, 141 (1983).
[59] R. Loudon and P. L. Knight, J. Mod. Opt. **34**, 709 (1987).
[60] M. Angelova, A. Hertz, and V. Hussin, J. Phys. A **45**, 244007 (2012).
[61] P. Kok, W. J. Munro, K. Nemoto, T. C. Ralph, J. P. Dowling, and G. J. Milburn, Rev. Mod. Phys. **79**, 135 (2007).
[62] P. Kok and B. W. Lovett, *Optical Quantum Information Processing* (Cambridge University Press, Cambridge, England, 2010).
[63] Y. Yamamoto and H. A. Haus, Rev. Mod. Phys. **58**, 1001 (1986).
[64] V. Giovannetti, S. Lloyd, and L. Maccone, Nat. Photonics **5**, 222 (2011).
[65] M. Hillery, Phys. Rev. A **61**, 022309 (2000).
[66] P. M. Anisimov, G. M. Raterman, A. Chiruvelli, W. N. Plick, S. D. Huver, H. Lee, and J. P. Dowling, Phys. Rev. Lett. **104**, 103602 (2010).
[67] J. Aasi *et al.*, Nat. Photonics **7**, 613 (2013).
[68] S. Ghosh and P. Roy, Phys. Lett. B **711**, 423 (2012).
[69] S. Dey and A. Fring, Phys. Rev. D **86**, 064038 (2012).
[70] P. Pedram, Int. J. Mod. Phys. D **22**, 1350004 (2013).
[71] S. Dey, Phys. Rev. D **91**, 044024 (2015).
[72] S. Dey, A. Fring, and V. Hussin, Springer Proc. Phys. **205**, 209 (2018).
[73] S. Dey and V. Hussin, Phys. Rev. D **91**, 124017 (2015).
[74] K. Zelaya, S. Dey, and V. Hussin, Phys. Lett. A **382**, 3369 (2018).
[75] E. M. F. Curado, M. A. Rego-Monteiro, and Ligia M. C. S. Rodrigues, Phys. Rev. A **87**, 052120 (2013).
[76] K. Berrada and H. Eleuch, Phys. Rev. D **100**, 016020 (2019).
[77] Y. Wu and X. Yang, Phys. Rev. D **73**, 067701 (2006).
[78] C. Quesne and N. Vansteenkiste, J. Phys. A **28**, 7019 (1995).
[79] E. M. F. Curado and M. A. Rego-Monteiro, J. Phys. A **34**, 3253 (2001).
[80] Y. Hassouni, E. M. F. Curado, and M. A. Rego-Monteiro, Phys. Rev. A **71**, 022104 (2005).

[81] J. P. Antoine, J. P. Gazeau, P. Monceau, J. R. Klauder, and K. A. Penson, J. Math. Phys. (N.Y.) **42**, 2349 (2001).
[82] J. R. Klauder, Ann. Phys. (N.Y.) **237**, 147 (1995).
[83] J. R. Klauder and J.-P. Gazeau, J. Phys. A **32**, 123 (1999).
[84] E. Schrodinger, Naturwissenschaften **14**, 664 (1926).
[85] W. M. Zhang, D. H. Feng, and R. Gilmore, Rev. Mod. Phys. **62**, 867 (1990).
[86] G. S. Agarwal and J. Benerji, Phys. Rev. A **64**, 023815 (2001).
[87] C. Quesne, J. Phys. A **35**, 9213 (2002).
[88] V. G. Drinfeld, in *Proceedings of the International Congress of Mathematicians, Berkeley, California, 1986* (American Mathematical Society, Providence, 1987), p. 798.
[89] E. Wigner, Phys. Rev. **77**, 711 (1950).
[90] L. M. Yang, Phys. Rev. **84**, 788 (1951).
[91] O. W. Greenberg, Phys. Rev. Lett. **13**, 598 (1964).
[92] M. S. Plyushchay, Phys. Lett. B **320**, 91 (1994).
[93] M. S. Plyushchay, Nucl. Phys. **B491**, 619 (1997).
[94] M. S. Plyushchay, Int. J. Mod. Phys. A **15**, 3679 (2000).
[95] P. A. Horváthy and M. S. Plyushchay, Phys. Lett. B **595**, 547 (2004).
[96] P. A. Horváthy, M. S. Plyushchay, and M. Valenzuela, Ann. Phys. (Amsterdam) **325**, 1931 (2010).
[97] M. S. Plyushchay, Ann. Phys. (N.Y.) **245**, 339 (1996).
[98] A. Dehghani, B. Mojaveri, S. Shirin, and M. Saedi, Ann. Phys. (Amsterdam) **362**, 659 (2015).
[99] A. Dehghani, B. Mojaveri, and S. A. Faseghandis, Mod. Phys. Lett. A **34**, 1950104 (2019).
[100] Sh. Dehdashti, M. B. Harouni, A. Mahdifar, and R. Roknizadeh, Laser Phys. **24**, 055203 (2014).
[101] A. Dehghani, B. Mojaveri, R. J. Bahrbeig, F. Nosrati, and R. L. Franco, J. Opt. Soc. Am. B **36**, 1858 (2019).
[102] A. Kempf, J. Math. Phys. (N.Y.) **35**, 4483 (1994).
[103] B. Bagchi and A. Fring, Phys. Lett. A **373**, 4307 (2009).
[104] J. J Sakurai and J. Napolitano, *Modern Quantum Mechanics* (Cambridge University Press, Cambridge, England, 2017).
[105] C. L. Ching, C. X. Yeo, and W. K. Ng, Int. J. Mod. Phys. A **32**, 1750009 (2017).
[106] R. K. Pathria, *Statistical Mechanics* (Butterworth Heinemann, Washington, DC, 1996).
[107] P. Bosso, S. Das, and R. B. Mann, Phys. Rev. D **96**, 066008 (2017).
[108] A. Kenfack and K. Zyczkowski, J. Opt. B **6**, 396 (2004).
[109] W. B. Case, Am. J. Phys. **76**, 937 (2008).
[110] A. Bassi, A. Grobardt, and H. Ulbricht, Classical Quantum Gravity **34**, 193002 (2017).
[111] I. Pokovski, M. Zych, F. Costa, and C. Brukner, Nat. Phys. **11**, 668 (2015).